NeuroImage 325 (2026) 121670

Contents lists available at ScienceDirect

NeuroImage

journal homepage: www.elsevier.com/locate/ynimg

Functional MRI following sensory stimulation in rat monosodium iodoacetate model of osteoarthritis pain as a tool for drug therapy discovery

Paula Lehtinen [a,*], Petteri Stenroos [b], Raimo Salo [b], Hennariikka Koivisto [b], Sami Virtanen [c], Hanne Laakso [b], Heikki Tanila [b], Andrii Domanskyi [c], Olli Gröhn [b], Carina Stenfors [c]

[a] Institute of Biomedicine, University of Turku, Turku, Finland
[b] A.I. Virtanen Institute for Molecular Sciences, University of Eastern Finland, Kuopio, Finland
[c] Orion Pharma, Orion Corporation, Turku, Finland

ARTICLE INFO

Keywords:
Osteoarthritis
Pain
Functional MRI
Pregabalin
Central pain processing

ABSTRACT

Chronic pain management in osteoarthritis (OA) remains a significant challenge, with current analgesic treatments often failing to provide adequate pain relief. A major issue in developing new therapies is the translational gap between preclinical animal models and clinical outcomes. This study investigates the use of functional magnetic resonance imaging (fMRI) to assess pain processing in the brain of a monosodium iodoacetate (MIA) -induced rat model of OA, combined with the pharmacological intervention of pregabalin (PGL). Thirty-two male Wistar rats were divided into sham and MIA groups, with the MIA group receiving intra-articular MIA injections to induce OA. Mechanical sensitivity was measured using the von Frey test, and fMRI was performed at baseline, on day 21, and post-PGL treatment on day 22. Results showed significant hypersensitivity in the MIA group by day 21, with altered brain activity in pain-related regions such as the thalamus and retrosplenial cortex. PGL treatment on day 22 significantly alleviated mechanical hypersensitivity and reduced brain activity in the pain-related regions, including the thalamus, frontal cortex, insula, and cingulate cortex. These findings suggest that fMRI can provide objective measures of pain processing and the efficacy of analgesic treatments in preclinical models, potentially bridging the gap between animal studies and clinical trials. The study highlights the potential of fMRI as a tool for drug discovery in chronic pain management, emphasizing the need for further research with different analgesics to fully understand its utility.

1. Introduction

Chronic pain management in osteoarthritis (OA) represents a significant unmet medical challenge. Despite the availability of treatments such as nonsteroidal anti-inflammatory drugs (NSAIDs), corticosteroids, and physical therapy, many patients endure persistent pain (Krishnamurthy et al., 2021). While opioids demonstrate efficacy in certain cases, the associated risk of addiction underscores the necessity for innovative therapeutic approaches. In 2020, OA affected approximately 595 million people worldwide, and the number of cases is projected to increase in the future. Among those aged 30 years or older, 14.8 % experienced OA. (Steinmetz et al., 2023). The pain experienced in OA is multifaceted, involving both nociceptive and neuropathic components, resulting in considerable variability in pain perception among patients (Dimitroulas et al., 2014).

OA pain is driven by both peripheral and central mechanisms. Joint damage and inflammation initiate peripheral nociceptive pathways, leading to the sensitization of nociceptors via mechanical and biochemical factors (Schaible et al., 2011). Prolonged activation of these pathways can cause central sensitization, amplifying pain signals in the spinal cord and brain. (Woolf, 2011). This increases pain responses, even in the absence of active joint inflammation, contributing to the complexity of OA pain. Conventional therapies primarily address peripheral inflammation, often leaving central pain amplification unmanaged, which frequently results in insufficient pain relief (Moseng et al., 2024).

The development of novel pain management strategies for OA is hindered by the limited translational relevance of preclinical animal models. Although these models provide valuable insights into joint degeneration and inflammation, they often fail to replicate the chronic and multifaceted nature of pain experienced by human patients (Sadler et al., 2022). Furthermore, many animal models lack objective measures

* Corresponding author at: Kiinamyllynkatu 10, 20520 Turku, Finland.
E-mail address: paula.k.lehtinen@utu.fi (P. Lehtinen).

https://doi.org/10.1016/j.neuroimage.2025.121670
Received 7 October 2025; Received in revised form 18 December 2025; Accepted 18 December 2025
Available online 18 December 2025

of chronic pain perception, thereby complicating the assessment of new treatments. This disparity between preclinical research findings and clinical results has contributed significantly to the high rate of failure of analgesic drugs in OA pain clinical trials. (Miller and Malfait, 2017; Mouraux et al., 2021; Yekkirala et al., 2017)

Advancements in neuroimaging, particularly functional magnetic resonance imaging (fMRI), present a promising approach for addressing translational challenges. By fMRI, the direct, non-invasive observation of pain-related brain activity is enabled, providing an objective assessment of OA-associated pain processing in both human subjects and animal models (Parks et al., 2011; Upadhyay et al., 2013). Research utilizing fMRI in human subjects has revealed that OA pain correlates with modified activity in brain regions such as the anterior cingulate cortex, prefrontal cortex, insula, and thalamus (Kulkarni et al., 2007). These findings substantiate that OA pain involves intricate central neural processes, beyond its peripheral manifestation.

The utilization of neuroimaging in animal models, specifically the monosodium iodoacetate (MIA) model of OA, has significantly advanced the understanding of pain mechanisms. This model, involving the chemical induction of OA through intra-articular injection of MIA, has been extensively employed for the study of OA-related pain (Combe et al., 2004; De Sousa Valente, 2019; Van der Kraan et al., 1989). The MIA model encompasses both inflammatory and neuropathic components, which vary according to the progression phase of the model. In the late phase, the neuropathic component becomes more prominent, making the gabapentinoid pregabalin (PGL) an effective reference compound for pharmacological screening in animals. PGL is also widely used to manage neuropathic pain in humans. (De Sousa Valente, 2019). While behavioral assays remain the conventional method for assessing pain in these models, the incorporation of fMRI provides a more comprehensive evaluation by capturing alterations in brain activity associated with chronic pain (Abaei et al., 2016; Malisza et al., 2003). This approach can potentially bridge the translational gap between preclinical and clinical research, offering a more profound understanding of how potential analgesics impact both peripheral and central pain mechanisms.

Our study aimed to investigate changes in OA-associated pain processing pathways in the brain using fMRI in an MIA-induced rat model of OA, combined with pharmacological intervention using PGL.

2. Methods

2.1. Animals

A total of 32 naïve male Wistar rats (RccHan®:WIST, Envigo), weighing 306–384 g at the start of the study were used. Rats were housed in controlled conditions (temperature 22 ± 2 °C, humidity 55 ± 15 %), and with a 12/12 h light-dark cycle; two animals per cage in individually ventilated cages and had free access to food (SDS RM1 (E) SQC, Special Diet Services Ltd, Witham, England) and tap water throughout the studies. The animals were acclimatized to handling, and the von Frey boxes for at least one week before starting the experiments. All studies were carried out in accordance with the EU Directive 2010/63/EU for animal experiments and were approved by the Regional State Administrative Agency of Southern Finland (approval number ESAVI/33,509/2023).

2.2. Study design and exclusion criteria

The animals were injected with MIA on day 0, and their response to analgesic pharmacological treatment (oral PGL) was assessed in the von Frey test and fMRI imaging on day 22. Mechanical sensitivity was assessed with the von Frey test on baseline (BL, from day −6 to day −1), day 4, day 21, and 165 min after PGL dosing on day 22. Functional MRI was performed on BL, day 21, and 210 min after PGL dosing on day 22. On day 22, following the last fMRI session, the animals were sacrificed (Fig. 1).

Two rats were excluded from the MIA group during the study for the even group size ($n = 10$ per group) on day 22. The rats excluded were non-sensitive based on the mechanical sensitivity measurement on day 21. Additionally, two rats, one from each MIA group, were excluded post hoc due to abnormally high mechanical hypersensitivity or lack of response to PGL treatment. Also, 8 individual fMRI baseline sessions were excluded due to frequency shifts (> 10 %/voxel size), caused by a wristwatch in the experimenter's hand during von Frey stimulation. Additionally, 4 sessions (2 sessions from D22 sham + vehicle group, 2 from D22 MIA + vehicle group) were excluded due to a wound in a paw after stimulation, which can cause some irrelevant pain signals. The distribution of animals in treatment groups is shown in Fig. 2.

Moreover, the results related to a stimulus using a 52 g filament (Optihair2) were excluded due to uncertainty in the filament alignment with the paw between two consecutive scans, which involved first using

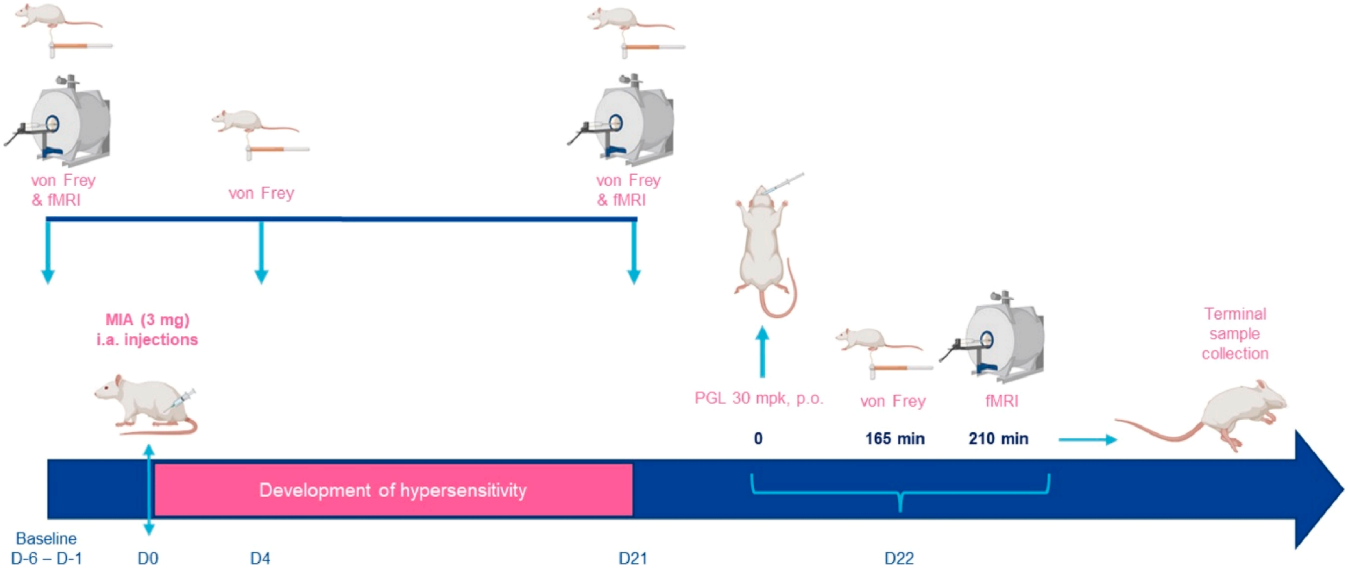

Fig. 1. Study design scheme. MIA = monosodium iodoacetate, fMRI = functional magnetic resonance imaging, PGL = pregabalin.

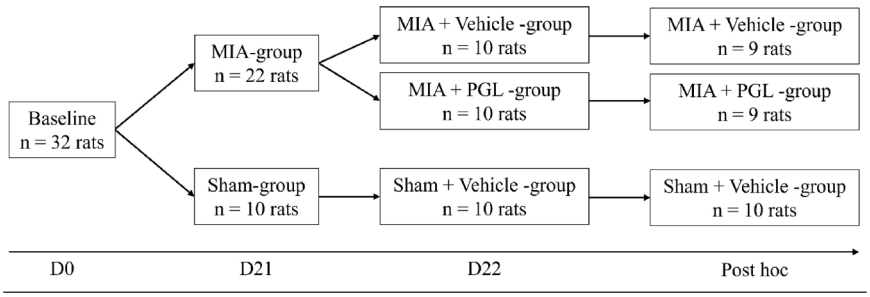

Fig. 2. Number of animals per group during the study. MIA = monosodium iodoacetate, PGL = pregabalin.

the 26 g filament and then the 52 g filament.

2.3. MIA model induction

MIA injections were done to 22 rats (MIA-group) while 10 rats (sham-group) were given saline on day 0 (Fig. 2). Under isoflurane anesthesia (isoflurane-oxygen mixture, induction 4 %, maintenance 2–3 %), the knee area of the right hind leg was shaved and disinfected. MIA (Sigma-Aldrich, cat #I2512; diluted in saline to 75 mg/ml concentration on the morning of injection; dosing 3 mg (40 µl)/animal) or saline (40 µl/animal of 0.9 % NaCl-solution; B. Braun, Melsungen, Germany) was injected intra-articularly into the knee joint.

2.4. Mechanical sensitivity

Mechanical sensitivity measurement with manual von Frey filament test was performed on BL, day 4, day 21, and day 22 post-dosing of PGL. Animals were first habituated to von Frey boxes for 5–10 min (or as long as they were settled down and not moving). The 50 % paw withdrawal threshold was determined from the plantar side of both hind paws with the up-and-down method (Chaplan et al., 1994; Dixon, 1980) using the Optihair2 filament series (MRC Systems, Germany). The test began with a 3.3 g filament and continued with filaments of increased or decreased forces depending on the response, with a maximum of nine applications. One filament was applied for up to 8 *sec*. The interval between the presentation of filaments was 5–10 s, or until the behavior evoked by the presentation of the filament had ceased.

2.5. Functional MRI

Imaging was performed under isoflurane-medetomidine anesthesia. Anesthesia was induced with 5 % isoflurane in an induction chamber, followed by 2 % in an animal holder. A medetomidine bolus (0.015 mg/kg, s.c., Domitor®, Orion Pharma, Espoo, Finland) was injected, and after 15 min a continuous infusion of medetomidine (0.03 mg/kg/h, s.c.) was started, and isoflurane maintenance level was adjusted to 0.75–1 %. Imaging was performed at a 7T MRI system (Bruker Pharmascan) operated with ParaVision 6.0.1. software.

Anatomic images were acquired before the fMRI scans with fast spin-echo sequence (T2-TurboRARE) with the following parameters: repetition time 4 s, echo spacing 16.1 ms, 8 echoes, effective echo time 40 ms, matrix size 256 × 256, field-of-view 30 × 30 mm, 30 slices of 0.5 mm thickness (resulting in 0.12 × 0.12 × 0.5 mm non-isotropic spatial resolution which was retained throughout the data processing), bandwidth of 36 kHz and number of averages 2.

With fMRI, standard gradient echo-planar-imaging (EPI) based protocol was acquired with the following parameters: repetition time 1 s, echo time 18 ms, matrix size 64 × 64, field-of-view 30 × 30 mm, 17 slices of 1 mm thickness (resulting in 0.47 × 0.47 × 1 mm spatial resolution), bandwidth of 200 kHz, flip angle 60° and scan duration of 640 repetitions (resulting 10 min 40 s). The manual stimulus with ~1 Hz frequency was used in a 20 s ON and 40 s OFF paradigm to the ipsilateral hind paw in two consecutive scans, using at first 26 g and then 52 g filaments (Optihair2). The stimulus was provided using MRI-compatible filament, an extension rod, and in-house 3D-printed (Zmorph 2.0 SX) holders for the Bruker rat bed (Fig. 3). Imaging was performed on BL, day 21, and after PGL dosing on day 22.

2.6. Pharmacological intervention

Results from mechanical sensitivity testing on day 21 were used as a pre-dose measurement to assure the effect of MIA. Animals were divided into groups of sham + vehicle ($n = 10$), MIA + vehicle ($n = 10$), and MIA + PGL ($n = 10$) (Fig. 2). On day 22, a single oral dose of vehicle (0.9 % NaCl-solution; B. Braun, Melsungen, Germany) or 30 mg/kg PGL ((*S*)-Pregabalin, Toronto Research Chemicals Inc., Canada; diluted in 0.9 % NaCl to 10 mg/ml) was delivered. Mechanical sensitivity was assessed using a manual von Frey test 2.67–2.75 h after vehicle/PGL administration. Imaging with fMRI was executed and the first stimulation was performed 3.17–3.47 h after vehicle/PGL administration.

2.7. Data analysis and statistics

Mechanical sensitivity data are presented as mean values ± SD and analyzed using GraphPad Prism Software 9.1.0. Both model progression and treatment effect were subjected to the Kruskal-Wallis test with Dunn's multiple comparison post-hoc.

MRI data were preprocessed and analyzed using Snakemake (Köster

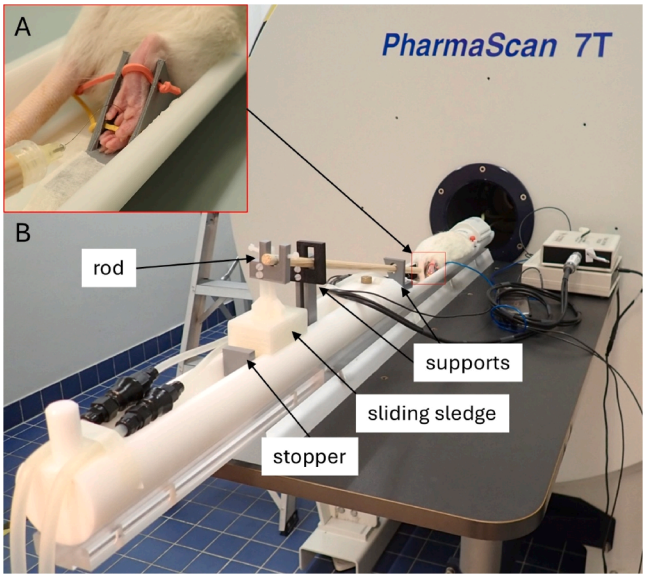

Fig. 3. Stimulation setup used during fMRI. Mechanical stimulation by the filament (A) was provided by moving a sliding sledge, where the von Frey rod was secured, between two stoppers (B) at ~1 Hz frequency. The rod was guided through two additional supports to be aligned with the center of the hind paw.

and Rahmann, 2012) and Python (version 3.10). First, data was converted from Bruker format to NIfTI using BrkRaw (Lee et al., 2020). Next, slice-timing correction (slicetimer, FSL) and motion correction using Advanced Normalization Tools (ANTs) (Avants et al., 2009) were applied. For normalization, images were co-registered to an anatomical T2-image reference acquired from the same study using ANTs with affine and non-linear SyN registration. Finally, spatial smoothing (0.6 voxel full-width at half-maximum Gaussian kernel, FSL) was applied. For statistical maps, the time series were high-pass filtered (0.01 Hz), autocorrelation was removed, and a general linear model (GLM) was used to estimate to goodness of fit of the stimulation period and fMRI signal. For GLM, stimulation ON/OFF periods were first modeled as boxcar function and then convolved with gamma-variate hemodynamic response function (HRF) assuming 6 s delay and 3 s variance using FSL FEAT (Woolrich et al., 2001). The obtained regressor was then used to estimate regression coefficient values (beta-values) for each voxel in the brain. Group-level statistical maps were generated separately for each planned contrast, including baseline, Day 21 (sham and MIA), Day 22 (sham + vehicle, MIA + vehicle, MIA + PGL), and the contrasts "Day 22 MIA + vehicle" versus "baseline" and "D22 - D21 MIA + PGL" versus "D22 - D21 MIA + vehicle. Each comparison was analyzed using Threshold-Free Cluster Enhancement (TFCE) and nonparametric permutation testing with family-wise error correction (Salimi-Khorshidi et al., 2011; Winkler et al., 2014). Voxel coordinates and multiple comparison corrected p-values of the local maximas within cluster were identified and reported (Suppl. Fig. 1). Additionally, we did correlation analyses between fMRI signal changes and behavioral responses. For fMRI, the response amplitude difference from the selected ROI was calculated between time points after and before PGL treatment. These values were plotted against the von Frey threshold differences calculated from the same animal for linear regression analysis. However, we did not find a statistically significant correlation in any of the ROIs (data not shown).

3. Results

3.1. Phenotype progression

The temporal progression of mechanical hypersensitivity was followed with the von Frey test at baseline and 4 and 21 days after model induction by MIA injections to the right knee. Paw withdrawal thresholds were similar before model induction in both paws (baseline (BL), Fig. 1A and B) in both sham and MIA groups. On day 4, variations in threshold values were seen in both groups. On the ipsilateral paw (Fig. 2B), the range was 7.6 ± 6.7 g in the sham group and 6.5 ± 4.3 g in the MIA group. Variations of a similar scale were also observed on day 21. However, on day 21, the MIA group showed significant hypersensitivity in the ipsilateral paw compared to the sham group and to the BL level of the MIA group, demonstrating successful model induction (Fig. 3B). Interestingly, an opposite development was observed in the withdrawal thresholds of the contralateral paw in the MIA group, with a significant hyposensitivity on day 21 compared to BL (Fig. 4A).

When sham and MIA groups were pooled together ($n = 24$), significant ($p < 0.05$, FWER corrected) fMRI activation in the contralateral somatosensory cortex was detected in response to 26 g stimulus before model induction (Fig. 5). While the sham group showed similar contralateral somatosensory activation on days 21 ($n = 9$) and 22 ($n = 8$), the only increased activation in the MIA group on day 21 ($n = 18$) was left-lateralized and included the mediodorsal, centrolateral, and laterodorsal thalamic nuclei. On day 22, the MIA group ($n = 8$) showed activation in the same left-lateralized thalamic regions as on D21, and, in addition, activation was seen bilaterally in the midline retrosplenial cortex.

When comparing the MIA group results on day 22 ($n = 8$) to all animals at the baseline ($n = 24$), significant differences were seen mainly in the thalamus and midbrain with a clear right lateralization. All animals were included in a comparison group to increase statistical power. Changes in the right thalamic region included the anterior, laterodorsal, mediodorsal, centrolateral, and ventrolateral nuclei as well as the habenula. The only increase in the left thalamus comprised the mediodorsal, centrolateral, and laterodorsal nuclei. In the midbrain, differences were seen in the midline superior colliculus and the right interior colliculus, periaqueductal gray, and cuneiform nucleus (Fig. 6).

3.2. Pregabalin effect

On day 22 post-MIA, the effect of PGL versus vehicle treatment on mechanical sensitivity was examined with the von Frey test. Day 21 results were used as a baseline based on which the MIA group was divided into two even groups, one receiving PGL and the other vehicle (Fig. 2). Before dosing, both MIA groups had significantly lower thresholds compared to sham and pre-MIA baseline (Figs. 4B and 7). After dosing, the MIA + PGL group showed significantly increased paw withdrawal threshold levels compared to the MIA + vehicle group. PGL treatment restored mechanical sensitivity thresholds to levels similar to the Sham + vehicle group. As expected, vehicle treatment had no effect

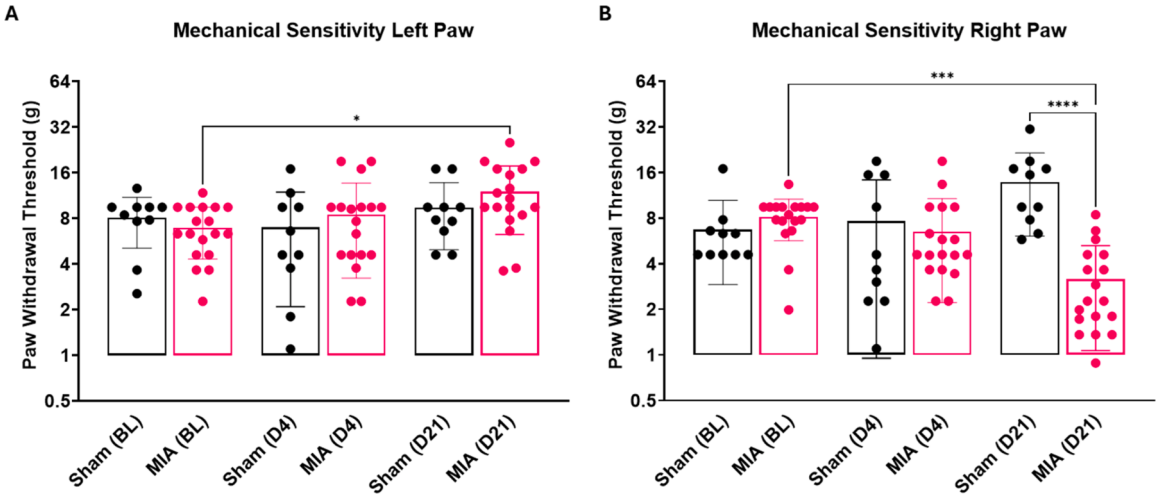

Fig. 4. Mechanical sensitivity of the left (A) and right (B) paw measured on baseline, day 4, and day 21 after model induction. Changes are shown as a 50 % withdrawal threshold for each hind paw. Results are shown as individual values and bars represent mean ± SD. Data were analyzed with the Kruskal-Wallis test with a Dunn's multiple comparison; *$p < 0.05$, ***$p < 0.001$, ****$p < 0.0001$. BL = baseline, MIA = monosodium iodoacetate.

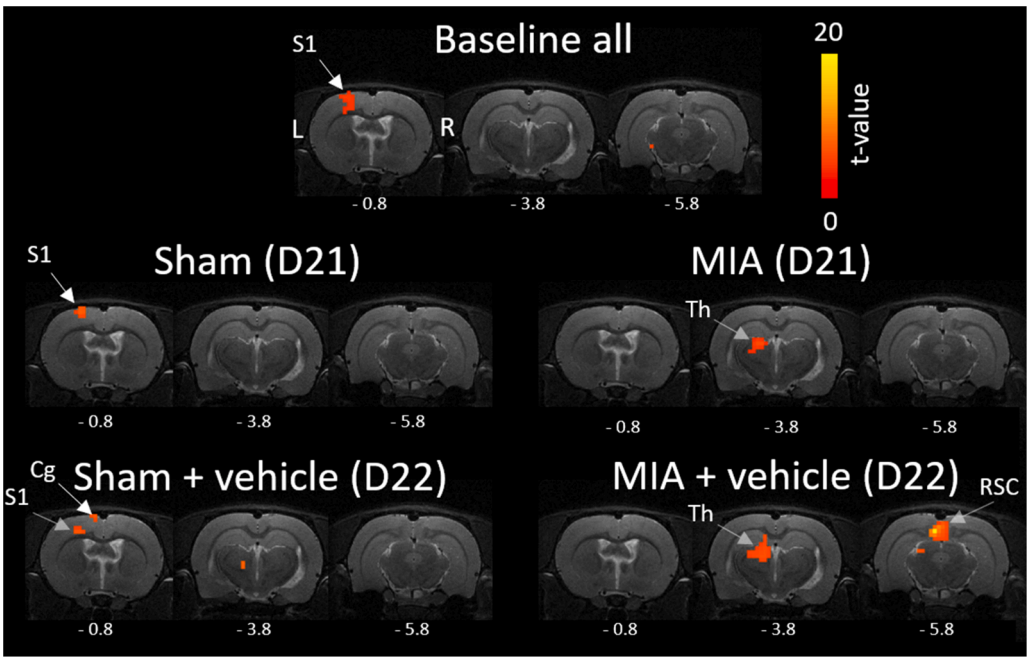

Fig. 5. Statistical maps of fMRI showing brain activation increase to 26 g stimulus in sham and MIA groups at the baseline ($n = 24$) and on days 21 ($n = 9$ sham, $n = 18$ MIA) and 22 ($n = 8$ sham, $n = 8$ MIA) after model induction. Significance was determined using a permutation test with p-values corrected for multiple comparisons using the family-wise error rate ($p < 0.05$). MIA = monosodium iodoacetate; S1 = somatosensory cortex, hind limb area; Cg = cingulate cortex; Th = thalamus, lateroposterior nucleus; RSC = retrosplenial cortex. The anterior-posterior coordinates below the brain slices are from Bregma.

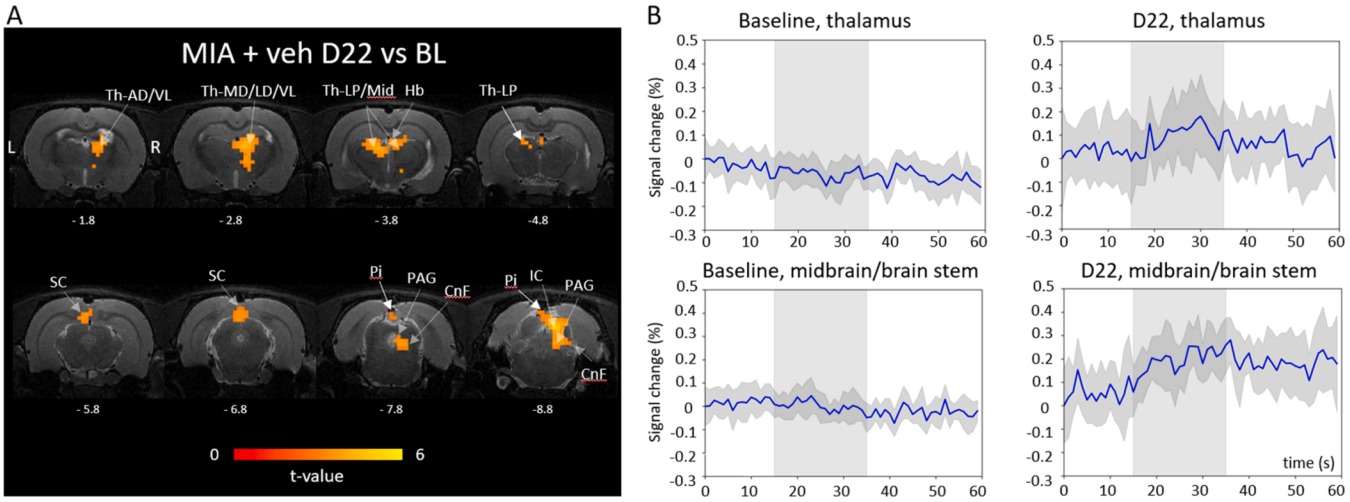

Fig. 6. (A) Statistical maps of fMRI and (B) average time series (±SD) from thalamus and midbrain/brain stem ROIs showing brain activation increases in the MIA group on D22 ($n = 8$) versus all animals at baseline ($n = 24$) in response to 26 g stimulus. Significance was determined using a permutation test with p-values corrected for multiple comparisons using the family-wise error rate ($p < 0.05$). MIA = monosodium iodoacetate; veh = vehicle; BL = baseline; Th = thalamus with specific nuclei: AD = anterodorsal, VL = ventrolateral, MD = mediodorsal, LD = laterodorsal, LP = lateroposterior, Mid = midline; Hb = habenula; SC = superior colliculus; Pi = pineal gland; PAG = Periaqueductal gray; CnF = cuneiform nucleus; IC = Inferior colliculus. The anterior-posterior coordinates below the brain slices are from Bregma.

on mechanical sensitivity in MIA + vehicle and Sham + vehicle animals (Fig. 7).

When comparing day 22 to day 21 results, a significant difference was seen between the MIA + vehicle ($n = 8$) and MIA + PGL ($n = 9$) groups ($p < 0.05$, FEWR corrected) in a broad network of midline and right-lateralized brain regions, with decreased activity in MIA + PGL groups. These regions included the entire medial frontal cortex, right insula, anterior and middle cingulate cortex, right medial striatum, right bed nucleus of the stria terminalis, left Cornu Ammonis 1, both habenulae, laterodorsal, mediodorsal and centrolateral thalamus on the right, centromedial thalamus bilaterally, left parafascicular nucleus, bilateral dorsal subiculum and right postsubiculum, inferior colliculus, right retrosplenial cortex, and right entorhinal cortex (Fig. 8). No differences were observed between the MIA + PGL and the Sham + vehicle groups ($p > 0.05$) post-treatment.

4. Discussion

In this study, the possibility of using fMRI as an objective functional readout for drug therapy discovery for chronic pain was investigated. The rat MIA model of OA was used and pain processing pathways in the brain were studied with fMRI followed by sensory stimulation.

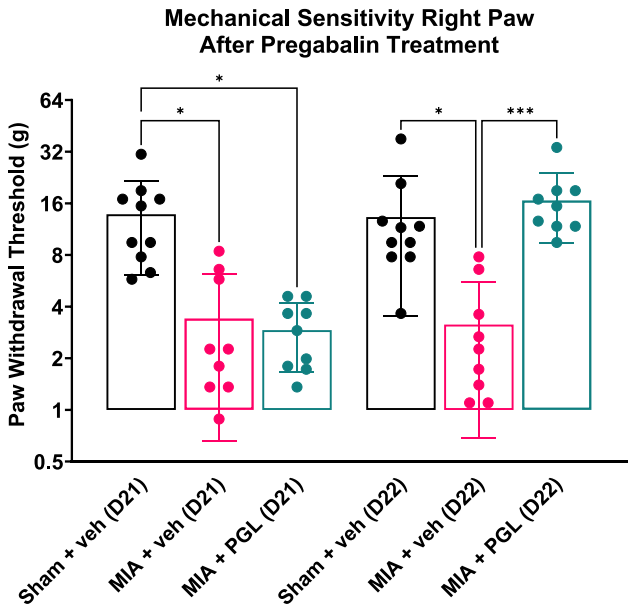

Fig. 7. Mechanical sensitivity of the right paw measured 2.67–2.75 h after pregabalin treatment. Changes are shown as a 50 % withdrawal threshold. Results are shown as individual values and on A bars represent mean ± SD. Results are shown as individual values and bars represent mean ± SD. Data were analyzed with the Kruskal-Wallis test with a Dunn's multiple comparison; $*p < 0.05$, $***p < 0.001$. BL = baseline, MIA = monosodium iodoacetate, PGL = pregabalin, veh = vehicle.

Mechanical sensitivity of rats was followed until the MIA group reached the state of hypersensitivity, after which the rats were treated with PGL.

Successful model induction was ensured by mechanical sensitivity testing. Hypersensitivity was reached in the MIA group 21 days after model induction. Interestingly, a difference was observed in the MIA group on the contralateral paw between BL and day 21 thresholds towards hyposensitivity. Development of contralateral hyposensitivity may indicate compensatory mechanisms involved in bilateral pain processing in osteoarthritis (Chaim et al., 2025; Pedersini et al., 2022). Additional studies need to be performed to clarify these mechanisms, which are beyond the scope of the present study. PGL delivered on day 22 alleviated pain-like behavioral phenotype in the MIA + PGL group, showing a significant increase in the paw withdrawal threshold post-treatment.

Pain processing involves several interconnected brain regions collectively called the neuromatrix of pain, first proposed by Melzack in 1999 (Melzack, 1999). This concept integrates both ascending and descending pathways. The primary and secondary somatosensory cortices as well as the insula, are part of the lateral ascending pathway, which mediates the sensory-discriminative aspects of pain. The thalamus plays a crucial role in transmitting pain signals to cortical areas. Medial components of the ascending pathway, such as the parabrachial nucleus, prefrontal cortex, anterior cingulate cortex, and amygdala, are responsible for affective and cognitive dimensions of pain. The descending pathway, involving structures such as the prefrontal cortex, anterior cingulate cortex, amygdala, hippocampus, hypothalamus, and periaqueductal gray, modulates nociceptive transmission from the medulla to the spinal cord. (Bushnell et al., 2013; Lithwick et al., 2013; Yao et al., 2023). Notably, the ascending pain pathways take a contralateral course, whereas the descending pathways are located ipsilaterally (Huang et al., 2019; Willis and Westlund, 1997).

Activation in the left-lateralized somatosensory cortex was observed in fMRI in both the MIA and sham groups at the baseline, indicating that this pattern was a result of mechanical stimulation with the filament. However, this activation was absent in the MIA group after day 21, possibly explained by high variability in fMRI responsiveness in the MIA group, demonstrating sensitization differences in the OA model. Instead, activation was detected in the left-lateralized thalamus and midline retrosplenial cortex. Interestingly, on day 22, the right-lateralized thalamus and midbrain (superior and inferior colliculi, cuneiform

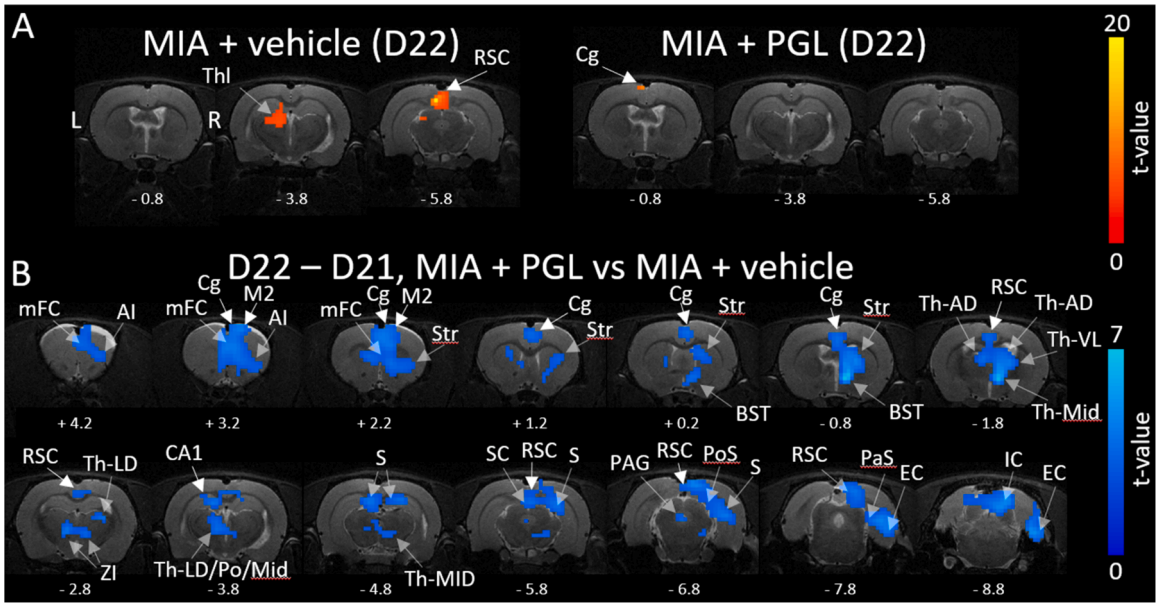

Fig. 8. Statistical maps of fMRI showing the effect of pregabalin treatment. (A) Statistical maps are presented from MIA groups on day 22 before (MIA + vehicle) and after pregabalin induction (MIA + PGL). (B) Differences were first calculated between D22 and D21 in all animals, then the MIA + vehicle group ($n = 8$) was compared to the MIA + PGL group ($n = 9$). Significantly reduced activity in animals treated with PGL was observed in several brain regions. Significance was determined using a permutation test with p-values corrected for multiple comparisons using the family-wise error rate ($p < 0.05$). MIA = monosodium iodoacetate; PGL - pregabalin; Cg = cingulate cortex; mFC = medial frontal cortex; AI = anterior insula; Str = striatum; BST = bed nucleus of stria terminalis; Th = thalamus with specific nuclei: LD = laterodorsal, AD = anterodorsal, Po posterior, mid = midline, VL = ventrolateral; CA1 = cornu ammonis of hippocampus; ZI = zona inserta; RSC = retrosplenial cortex; *S* = subiculum; PoS = post-subiculum; PaS = parasubiculum; PAG = Periaqueductal gray; EC = entorhinal cortex; SC = superior colliculus; IC = inferior colliculus; The anterior-posterior coordinates below the brain slices are from Bregma.

nucleus, and periaqueductal gray) were activated in the MIA group when comparing their results to all animals before model induction.

Thalamic activation observed in the MIA group after day 21 is reasonable as nociceptive signals must pass through the thalamus to reach their destination, whether in somatosensory or limbic regions of the brain. The thalamus was activated in the mediodorsal, centrolateral, and laterodorsal nuclei, indicating that signals are relayed through the medial spinothalamic tract, which is mostly associated with nociceptive-specific responses and emotional and affective aspects of pain (Groh et al., 2017; Lenz et al., 2024). Furthermore, chronic pain is often linked to structural and functional changes in the thalamus. These changes can include alterations in thalamic connectivity, which may play a role in the persistence of chronic pain (Groh et al., 2018). As the MIA group exhibited decreased activity in the somatosensory cortex after day 21, thalamic connectivity might be somewhat dysfunctional. Previous human studies indicate abnormal connectivity between the thalamus and the somatosensory cortex, as well as between the thalamus and the insula, which contribute to sensory and affective pain processing (Cauda et al., 2009; Tu et al., 2020). The changes are related to thalamocortical dysrhythmia, which is marked by disrupted oscillatory activity and decreased inhibitory tone (Schulman et al., 2005; Yan et al., 2023).

Interestingly, the changes observed on day 22 were mainly right-lateralized. Ipsilateral pain lateralization in the brain has been noted in conditions such as allodynia, hyperalgesia, neuropathic, and chronic pain (Hashmi et al., 2013; Lanz et al., 2011; Peyron et al., 2004), all of which are also expressed in the MIA model. Furthermore, ipsilateral pain lateralization in the brain is linked to pain processing and controlling (Hashmi et al., 2013; Roza and Martinez-Padilla, 2021). This phenomenon and bilateral activation have also been seen in previous pain-related in vivo fMRI studies (Abaei et al., 2016; Malisza et al., 2003).

Activation in the superior and inferior colliculi as well as in the cuneiform nucleus was observed in the MIA group, highlighting their involvement despite not being traditionally listed among the brain regions associated with the pain neuromatrix. In rodents, these regions interact with the periaqueductal gray, which is an integral part of the descending pain signaling pathway. The periaqueductal gray plays a crucial role in integrating sensory information from the superior and inferior colliculi and cuneiform nucleus, and modulating responses, including pain. (Chang et al., 2020; Freitas et al., 2005). Both colliculi and the cuneiform nucleus are also connected to each other and also to the thalamus (Cauzzo et al., 2022; Chang et al., 2020). Moreover, activation of the superior colliculus in response to noxious mechanical stimuli has been shown in various pain models (Moylan Governo et al., 2006; Spisák et al., 2017), including the MIA model (Abaei et al., 2016).

PGL treatment on day 22 produced a significant effect when comparing the MIA groups, with the MIA + PGL group exhibiting reduced activity in the midline or several right-lateralized brain regions associated with pain. Reduced activity in fMRI in MIA + PGL animals to the levels observed in the Sham + vehicle group was associated with attenuated mechanical hypersensitivity after PGL treatment. The effect of PGL as a reduced activity was significant in pain-related brain regions from the descending pathway, such as the frontal cortex, cingulate cortex, insula, bed nucleus of the stria terminalis, and multiple thalamic regions. In addition, the activity of the right-lateralized striatum, retrosplenial, and entorhinal cortex was reduced by PGL. These regions have previously been linked to chronic pain (Borsook et al., 2010; Hao et al., 2025; Ploghaus et al., 2001). Activity from all of these regions reduced by PGL primarily relates to the emotional aspects of pain signaling. Additionally, the right-lateralization suggests that PGL can reduce the need for pain processing and controlling. However, follow-up studies with different analgesics will be needed to understand the utility of fMRI for measuring the affective component of pain in MIA-treated rats.

Anesthetics are known to influence brain resting state activity (Paasonen et al., 2018), stimulus responses (Paasonen et al., 2016) and hemodynamic responses (Martin et al., 2006). In addition, medetomidine also affects the cardiovascular system, can cause hypothermia, and reduces cerebral blood flow (Sinclair, 2003). However, the negative effects of medetomidine anesthesia can be mitigated by using isoflurane-medetomidine combination anesthesia, preserving biologically plausible functional connectivity patterns (Grandjean et al., 2023a, 2023b; Paasonen et al., 2018). Moreover, a very low concentration of medetomidine (only 0.03 mg/kg/h) was used to minimize its known pain-alleviating effects (Siegenthaler et al., 2020).

The effect of anesthesia and using PGL as a pain treatment can be considered as limitations in this study. Due to the pain-alleviation effects of medetomidine, reduced functional responses can be possible in pain pathways involving regions like the somatosensory, cingulate cortices, and thalamus. As isoflurane-medetomidine anesthesia especially affects subcortical-subcortical and cortico-subcortical synchrony (Paasonen et al., 2018), fMRI responses in these brain connections can also be hindered. Additionally, PGL's sedative effects can result in drowsiness and dizziness. However, it primarily functions as a painkiller and secondarily as a sedative, as documented in clinical studies (Karube et al., 2017). Lastly, although PGL can have a minor effect on blood pressure and heart rate (Hao et al., 2025), we cannot completely rule out the possibility of altered hemodynamics influencing our results. Distortion correction was not applied in data analysis. Although distortions and signal dropouts can be problematic in echo-planar imaging, particularly near air-tissue interfaces, these artefacts were not pronounced in our data. Importantly, the observed functional responses did not co-localize with regions typically prone to such artefacts.

This study shows the potential of fMRI as an objective tool for pain drug therapy discovery. The MIA model demonstrated logical pain-related activation patterns, and PGL treatment was able to reduce those to the level of sham animals. To expand our knowledge about the sensitivity and utility of fMRI in measuring different aspects of pain sensation and processing, other analgesic compounds need to be tested. Compared to PGL, which is mostly used for treating neuropathic pain, a better and more targeted treatment could be Tanezumab which has promising results in the treatment of chronic musculoskeletal pain conditions (Jayabalan and Schnitzer, 2017). In addition, it would be worthwhile to explore the potential of dual fMRI of the brain and spinal cord to visualize the central and peripheral pain processing pathways simultaneously.

CRediT authorship contribution statement

Paula Lehtinen: Writing – review & editing, Writing – original draft, Visualization, Methodology, Investigation, Conceptualization. **Petteri Stenroos:** Writing – review & editing, Writing – original draft, Visualization, Validation, Methodology, Investigation. **Raimo Salo:** Formal analysis. **Hennariikka Koivisto:** Investigation, Formal analysis. **Sami Virtanen:** Formal analysis. **Hanne Laakso:** Writing – review & editing. **Heikki Tanila:** Writing – review & editing, Supervision. **Andrii Domanskyi:** Writing – review & editing, Supervision, Conceptualization. **Olli Gröhn:** Writing – review & editing, Methodology. **Carina Stenfors:** Writing – review & editing, Conceptualization.

Declaration of competing interest

Authors Domanskyi Andrii and Stenfors Carina are employees of a pharmaceutical company (Orion Pharma). Other authors have no conflict of interest.

Acknowledgment

The authors want to acknowledge the Lab Animal Centre of the University of Eastern Finland for taking care of the animals during this study and Sara Häkli for being part of the pilot studies. The computation was performed on servers provided by the UEF Bioinformatics Center,

University of Eastern Finland, Finland.

Supplementary materials

Supplementary material associated with this article can be found, in the online version, at doi:10.1016/j.neuroimage.2025.121670.

References

Abaei, M., Sagar, D.R., Stockley, E.G., Spicer, C.H., Prior, M., Chapman, V., Auer, D.P., 2016. Neural correlates of hyperalgesia in the monosodium iodoacetate model of osteoarthritis pain. Mol. Pain. 12. https://doi.org/10.1177/1744806916642445.

Avants, B., Tustison, N., Johnson, H., 2009. Advanced Normalization Tools (ANTS). Insight J.

Borsook, D., Upadhyay, J., Chudler, E.H., Becerra, L., 2010. A key role of the basal ganglia in pain and analgesia - insights gained through human functional imaging. Mol. Pain. 6. https://doi.org/10.1186/1744-8069-6-27.

Bushnell, M.C., Čeko, M., Low, L.A., 2013. Cognitive and emotional control of pain and its disruption in chronic pain. Nat. Rev. Neurosci. 14 (7). https://doi.org/10.1038/nrn3516.

Cauda, F., Sacco, K., D'Agata, F., Duca, S., Cocito, D., Geminiani, G., Migliorati, F., Isoardo, G., 2009. Low-frequency BOLD fluctuations demonstrate altered thalamocortical connectivity in diabetic neuropathic pain. BMC Neurosci. 10. https://doi.org/10.1186/1471-2202-10-138.

Cauzzo, S., Singh, K., Stauder, M., García-Gomar, M.G., Vanello, N., Passino, C., Staab, J., Indovina, I., Bianciardi, M., 2022. Functional connectome of brainstem nuclei involved in autonomic, limbic, pain and sensory processing in living humans from 7 Tesla resting state fMRI. Neuroimage 250. https://doi.org/10.1016/j.neuroimage.2022.118925.

Chaim, F.F., Imamura, M., Chaim-Avancini, T.M., Leite, C.C., Squarzoni, P., Battistella, L. R., Fregni, F., 2025. Brain compensation and volume alterations in patients with severe knee osteoarthritis: a cross-sectional neuroimaging study. Rheumatol. Int. 45 (9), 198. https://doi.org/10.1007/s00296-025-05929-w.

Chang, S.J., Cajigas, I., Opris, I., Guest, J.D., Noga, B.R., 2020. Dissecting Brainstem Locomotor Circuits: converging Evidence for Cuneiform Nucleus Stimulation. Front. Syst. Neurosci. 14. https://doi.org/10.3389/fnsys.2020.00064.

Chaplan, S.R., Bach, F.W., Pogrel, J.W., Chung, J.M., Yaksh, T.L., 1994. Quantitative assessment of tactile allodynia in the rat paw. J. Neurosci. Methods 53 (1). https://doi.org/10.1016/0165-0270(94)90144-9.

Combe, R., Bramwell, S., Field, M.J., 2004. The monosodium iodoacetate model of osteoarthritis: a model of chronic nociceptive pain in rats? Neurosci. Lett. 370 (2–3). https://doi.org/10.1016/j.neulet.2004.08.023.

De Sousa Valente, J., 2019. The pharmacology of pain associated with the monoiodoacetate model of osteoarthritis. Front. Pharmacol. 10. https://doi.org/10.3389/fphar.2019.00974.

Dimitroulas, T., Duarte, R.V., Behura, A., Kitas, G.D., Raphael, J.H., 2014. Neuropathic pain in osteoarthritis: a review of pathophysiological mechanisms and implications for treatment. Semin. Arthritis Rheum. 44 (2). https://doi.org/10.1016/j.semarthrit.2014.05.011.

Dixon, W.J., 1980. Efficient analysis of experimental observations. Annu. Rev. Pharmacol. Toxicol. 20. https://doi.org/10.1146/annurev.pa.20.040180.002301.

Freitas, R.L., Ferreira, C.M.R., Ribeiro, S.J., Carvalho, A.D., Elias-Filho, D.H., Garcia-Cairasco, N., Coimbra, N.C., 2005. Intrinsic neural circuits between dorsal midbrain neurons that control fear-induced responses and seizure activity and nuclei of the pain inhibitory system elaborating postictal antinociceptive processes: a functional neuroanatomical and neuropharmacological study. Exp. Neurol. 191 (2). https://doi.org/10.1016/j.expneurol.2004.10.009.

Grandjean, J., Desrosiers-Gregoire, G., Anckaerts, C., Angeles-Valdez, D., Ayad, F., Barrière, D.A., Blockx, I., Bortel, A., Broadwater, M., Cardoso, B.M., Célestine, M., Chavez-Negrete, J.E., Choi, S., Christiaen, E., Clavijo, P., Colon-Perez, L., Cramer, S., Daniele, T., Dempsey, E., Hess, A., 2023a. A consensus protocol for functional connectivity analysis in the rat brain. Nat. Neurosci. 26 (4). https://doi.org/10.1038/s41593-023-01286-8.

Grandjean, J., Desrosiers-Gregoire, G., Anckaerts, C., Angeles-Valdez, D., Ayad, F., Barrière, D.A., Blockx, I., Bortel, A., Broadwater, M., Cardoso, B.M., Célestine, M., Chavez-Negrete, J.E., Choi, S., Christiaen, E., Clavijo, P., Colon-Perez, L., Cramer, S., Daniele, T., Dempsey, E., Hess, A., 2023b. Author Correction: a consensus protocol for functional connectivity analysis in the rat brain. Nat. Neurosci. (6), 26. https://doi.org/10.1038/s41593-023-01328-1.

Groh, A., Krieger, P., Mease, R.A., Henderson, L., 2018. Acute and Chronic Pain Processing in the Thalamocortical System of Humans and Animal Models. Neuroscience 387. https://doi.org/10.1016/j.neuroscience.2017.09.042.

Groh, A., Mease, R.A., Krieger, P., 2017. Pain processing in the thalamocortical system. Neuroforum. 23 (3). https://doi.org/10.1515/nf-2017-A019.

Hao, S., Xue, M., Chen, Q.-Y., Wan, J., Ma, Y.-J., Shi, W., Chen, X., Li, X.-H., Lu, J.-S., Xu, F., Bi, G.-Q., Tao, W., Zhuo, M., 2025. Supraspinal facilitation of painful stimuli by glutamatergic innervation from the retrosplenial to the anterior cingulate cortex. PLoS Biol. 23 (1), e3003011. https://doi.org/10.1371/journal.pbio.3003011.

Hashmi, J.A., Baliki, M.N., Huang, L., Baria, A.T., Torbey, S., Hermann, K.M., Schnitzer, T.J., Apkarian, A.V., 2013. Shape shifting pain: chronification of back pain shifts brain representation from nociceptive to emotional circuits. Brain (9), 136. https://doi.org/10.1093/brain/awt211.

Huang, J., Gadotti, V.M., Chen, L., Souza, I.A., Huang, S., Wang, D., Ramakrishnan, C., Deisseroth, K., Zhang, Z., Zamponi, G.W., 2019. A neuronal circuit for activating descending modulation of neuropathic pain. Nat. Neurosci. (10), 22. https://doi.org/10.1038/s41593-019-0481-5.

Jayabalan, P., Schnitzer, T.J., 2017. Tanezumab in the treatment of chronic musculoskeletal conditions. Expert. Opin. Biol. Ther. 17 (2). https://doi.org/10.1080/14712598.2017.1271873.

Karube, N., Ito, S., Sako, S., Hirokawa, J., Yokoyama, T., 2017. Sedative effects of oral pregabalin premedication on intravenous sedation using propofol target-controlled infusion. J. Anesth. 31 (4). https://doi.org/10.1007/s00540-017-2366-7.

Köster, J., Rahmann, S., 2012. Snakemake-a scalable bioinformatics workflow engine. Bioinformatics (19), 28. https://doi.org/10.1093/bioinformatics/bts480.

Krishnamurthy, A., Lang, A.E., Pangarkar, S., Edison, J., Cody, J., & Sall, J. (2021). Synopsis of the 2020 US Department of Veterans Affairs/US Department of Defense Clinical Practice Guideline: the Non-Surgical Management of Hip and Knee Osteoarthritis. In *Mayo Clinic Proceedings* (Vol. 96, Issue 9). https://doi.org/10.1016/j.mayocp.2021.03.017.

Kulkarni, B., Bentley, D.E., Elliott, R., Julyan, P.J., Boger, E., Watson, A., Boyle, Y., El-Deredy, W., Jones, A.K.P., 2007. Arthritic pain is processed in brain areas concerned with emotions and fear. Arthritis Rheum. 56 (4). https://doi.org/10.1002/art.22460.

Lanz, S., Seifert, F., Maihöfner, C., 2011. Brain activity associated with pain, hyperalgesia and allodynia: an ALE meta-analysis. J. Neural. Transm. 118 (8). https://doi.org/10.1007/s00702-011-0606-9.

Lee, S.-H., Ban, W., Shih, Y.-Y.I., 2020. *BrkRaw/bruker: BrkRaw v0.3.3 (0.3.3)* (0.3.3). Zenodo. https://doi.org/10.5281/zenodo.3877179.

Lenz, F.A., Dougherty, P.M., Meeker, T.J., Saffer, M.I., Oishi, K., 2024. Neuroscience of the human thalamus related to acute pain and chronic "thalamic" pain. J. Neurophysiol. 132 (6), 1756–1778. https://doi.org/10.1152/jn.00065.2024.

Lithwick, A., Lev, S., Binshtok, A.M., 2013. Chronic Pain-Related Remodeling of Cerebral Cortex - 'Pain Memory': a Possible Target for Treatment of Chronic Pain. Pain. Manage 3 (1). https://doi.org/10.2217/pmt.12.74.

Malisza, K.L., Gregorash, L., Turner, A., Foniok, T., Stroman, P.W., Allman, A.A., Summers, R., Wright, A., 2003. Functional MRI involving painful stimulation of the ankle and the effect of physiotherapy joint mobilization. Magn. Reson. Imaging 21 (5). https://doi.org/10.1016/S0730-725X(03)00074-2.

Martin, C., Martindale, J., Berwick, J., Mayhew, J., 2006. Investigating neural-hemodynamic coupling and the hemodynamic response function in the awake rat. Neuroimage (1), 32. https://doi.org/10.1016/j.neuroimage.2006.02.021.

Melzack, R., 1999. From the gate to the neuromatrix. Pain 82 (SUPPL.1). https://doi.org/10.1016/S0304-3959(99)00145-1.

Miller, R.E., & Malfait, A.M. (2017). Osteoarthritis pain: what are we learning from animal models? In *Best Practice and Research: Clinical Rheumatology* (Vol. 31, Issue 5). https://doi.org/10.1016/j.berh.2018.03.003.

Moseng, T., Vliet Vlieland, T.P.M., Battista, S., Beckwée, D., Boyadzhieva, V., Conaghan, P.G., Costa, D., Doherty, M., Finney, A.G., Georgiev, T., Gobbo, M., Kennedy, N., Kjeken, I., Kroon, F.P.B., Lohmander, L.S., Lund, H., Mallen, C.D., Pavelka, K., Pitsillidou, I.A., Østerås, N., 2024. EULAR recommendations for the non-pharmacological core management of hip and knee osteoarthritis: 2023 update. Ann. Rheum. Dis. 83 (6). https://doi.org/10.1136/ard-2023-225041.

Mouraux, A., Bannister, K., Becker, S., Finn, D.P., Pickering, G., Pogatzki-Zahn, E., Graven-Nielsen, T., 2021. Challenges and opportunities in translational pain research - An opinion paper of the working group on translational pain research of the European pain federation (EFIC). Eur. J. Pain (U. K.) (4), 25. https://doi.org/10.1002/ejp.1730.

Moylan Governo, R.J., Morris, P.G., William Prior, M.J., Marsden, C.A., Chapman, V., 2006. Capsaicin-evoked brain activation and central sensitization in anaesthetised rats: a functional magnetic resonance imaging study. Pain 126 (1–3). https://doi.org/10.1016/j.pain.2006.06.012.

Paasonen, J., Salo, R.A., Shatillo, A., Forsberg, M.M., Närväinen, J., Huttunen, J.K., Gröhn, O., 2016. Comparison of seven different anesthesia protocols for nicotine pharmacologic magnetic resonance imaging in rat. Eur. Neuropsychopharmacol. 26 (3). https://doi.org/10.1016/j.euroneuro.2015.12.034.

Paasonen, J., Stenroos, P., Salo, R.A., Kiviniemi, V., Gröhn, O., 2018. Functional connectivity under six anesthesia protocols and the awake condition in rat brain. Neuroimage 172. https://doi.org/10.1016/j.neuroimage.2018.01.014.

Parks, E.L., Geha, P.Y., Baliki, M.N., Katz, J., Schnitzer, T.J., Apkarian, A.V., 2011. Brain activity for chronic knee osteoarthritis: dissociating evoked pain from spontaneous pain. Eur. J. Pain (8), 15. https://doi.org/10.1016/j.ejpain.2010.12.007.

Pedersini, P., Gobbo, M., Bishop, M.D., Arendt-Nielsen, L., Villafañe, J.H., 2022. Functional and Structural Neuroplastic Changes Related to Sensitization Proxies in Patients with Osteoarthritis: a Systematic Review. Pain Med. (U. S.) 23 (3). https://doi.org/10.1093/pm/pnab301.

Peyron, R., Schneider, F., Faillenot, I., Convers, P., Barral, F.G., Garcia-Larrea, L., Laurent, B., 2004. An fMRI study of cortical representation of mechanical allodynia in patients with neuropathic pain. Neurology (10), 63. https://doi.org/10.1212/01.WNL.0000144177.61125.85.

Ploghaus, A., Narain, C., Beckmann, C.F., Clare, S., Bantick, S., Wise, R., Matthews, P.M., Nicholas P Rawlins, J., Tracey, I., 2001. Exacerbation of pain by anxiety is associated with activity in a hippocampal network. J. Neurosci. 21 (24). https://doi.org/10.1523/jneurosci.21-24-09896.2001.

Roza, C., Martinez-Padilla, A., 2021. Asymmetric lateralization during pain processing. In: Symmetry, 13. https://doi.org/10.3390/sym13122416.

Sadler, K.E., Mogil, J.S., Stucky, C.L., 2022. Innovations and advances in modelling and measuring pain in animals. Nat. Rev. Neurosci. 23 (2). https://doi.org/10.1038/s41583-021-00536-7.

Salimi-Khorshidi, G., Smith, S.M., Nichols, T.E., 2011. Adjusting the effect of nonstationarity in cluster-based and TFCE inference. Neuroimage (3), 54. https://doi.org/10.1016/j.neuroimage.2010.09.088.

Schaible, H.G., Ebersberger, A., & Natura, G. (2011). Update on peripheral mechanisms of pain: beyond prostaglandins and cytokines. In *Arthritis Research and Therapy* (Vol. 13, Issue 2). https://doi.org/10.1186/ar3305.

Schulman, J.J., Ramirez, R.R., Zonenshayn, M., Ribary, U., Llinas, R., 2005. Thalamocortical dysrhythmia syndrome: MEG imaging of neuropathic pain. Thalamus Relat. Syst. 3 (1). https://doi.org/10.1017/S1472928805000063.

Siegenthaler, J., Pleyers, T., Raillard, M., Spadavecchia, C., Levionnois, O.L., 2020. Effect of medetomidine, dexmedetomidine, and their reversal with atipamezole on the nociceptive withdrawal reflex in beagles. Animals (7), 10. https://doi.org/10.3390/ani10071240.

Sinclair, M.D. (2003). A review of the physiological effects of α2-agonists related to the clinical use of medetomidine in small animal practice. In *Canadian Veterinary Journal* (Vol. 44, Issue 11).

Spisák, T., Pozsgay, Z., Aranyi, C., Dávid, S., Kocsis, P., Nyitrai, G., Gajári, D., Emri, M., Czurkó, A., Kincses, Z.T., 2017. Central sensitization-related changes of effective and functional connectivity in the rat inflammatory trigeminal pain model. Neuroscience 344. https://doi.org/10.1016/j.neuroscience.2016.12.018.

Steinmetz, J.D., Culbreth, G.T., Haile, L.M., Rafferty, Q., Lo, J., Fukutaki, K.G., Cruz, J.A., Smith, A.E., Vollset, S.E., Brooks, P.M., Cross, M., Woolf, A.D., Hagins, H., Abbasi-Kangevari, M., Abedi, A., Ackerman, I.N., Amu, H., Antony, B., Arabloo, J., Kopec, J. A., 2023. Global, regional, and national burden of osteoarthritis, 1990-2020 and projections to 2050: a systematic analysis for the Global Burden of Disease Study 2021. Lancet Rheumatol. 5 (9). https://doi.org/10.1016/S2665-9913(23)00163-7.

Tu, Y., Fu, Z., Mao, C., Falahpour, M., Gollub, R.L., Park, J., Wilson, G., Napadow, V., Gerber, J., Chan, S.T., Edwards, R.R., Kaptchuk, T.J., Liu, T., Calhoun, V., Rosen, B., Kong, J., 2020. Distinct thalamocortical network dynamics are associated with the pathophysiology of chronic low back pain. Nat. Commun. 11 (1). https://doi.org/10.1038/s41467-020-17788-z.

Upadhyay, J., Baker, S.J., Rajagovindan, R., Hart, M., Chandran, P., Hooker, B.A., Cassar, S., Mikusa, J.P., Tovcimak, A., Wald, M.J., Joshi, S.K., Bannon, A., Medema, J.K., Beaver, J., Honore, P., Kamath, R.V., Fox, G.B., Day, M., 2013. Pharmacological modulation of brain activity in a preclinical model of osteoarthritis. Neuroimage (1), 64. https://doi.org/10.1016/j.neuroimage.2012.08.084.

Van der Kraan, P.M., Vitters, E.L., Van de Putte, L.B.A., Van den Berg, W.B, 1989. Development of osteoarthritic lesions in mice by “metabolic” and “mechanical” alterations in the knee joints. Am. J. Pathol. 135 (6).

Willis, W.D., Westlund, K.N., 1997. Neuroanatomy of the pain system and of the pathways that modulate pain. J. Clin. Neurophysiol. 14 (1). https://doi.org/10.1097/00004691-199701000-00002.

Winkler, A.M., Ridgway, G.R., Webster, M.A., Smith, S.M., Nichols, T.E., 2014. Permutation inference for the general linear model. Neuroimage 92. https://doi.org/10.1016/j.neuroimage.2014.01.060.

Woolf, C.J., 2011. Central sensitization: implications for the diagnosis and treatment of pain. Pain 152 (SUPPL.3). https://doi.org/10.1016/j.pain.2010.09.030.

Woolrich, M.W., Ripley, B.D., Brady, M., Smith, S.M., 2001. Temporal autocorrelation in univariate linear modeling of FMRI data. Neuroimage (6), 14. https://doi.org/10.1006/nimg.2001.0931.

Yan, Y., Zhu, M., Cao, X., Xu, G., Shen, W., Li, F., Zhang, J., Luo, L., Zhang, X., Zhang, D., Liu, T., 2023. Thalamocortical Circuit Controls Neuropathic Pain via Up-regulation of HCN2 in the Ventral Posterolateral Thalamus. Neurosci. Bull. (5), 39. https://doi.org/10.1007/s12264-022-00989-5.

Yao, D., Chen, Y., & Chen, G. (2023). The role of pain modulation pathway and related brain regions in pain. *Reviews in the Neurosciences*. https://doi.org/10.1515/revneuro-2023-0037.

Yekkirala, A.S., Roberson, D.P., Bean, B.P., Woolf, C.J., 2017. Breaking barriers to novel analgesic drug development. Nat. Rev. Drug Discov. 16 (8). https://doi.org/10.1038/nrd.2017.87.